

Supporting Information

Surprising acidity of hydrated lithium cations in organic solvents

Haiqiang Deng,^a Pekka Peljo,^{a,b} T. Jane Stockmann,^a Liang Qiao,^a Tuomas Vainikka,^b Kyösti Kontturi,^b Marcin Opallo,^c and Hubert H. Girault^{a,*}

^a Laboratoire d'Electrochimie Physique et Analytique, Ecole Polytechnique Fédérale de Lausanne (EPFL), Station 6, CH-1015 Lausanne, Switzerland

^b Department of Chemistry, Aalto University, P.O. Box 16100, 00076, Finland

^c Institute of Physical Chemistry, Polish Academy of Sciences, ul. Kasprazaka 44/52, 01-224 Warszawa, Poland

* CORRESPONDING AUTHOR FOOTNOTE

E-mail: hubert.girault@epfl.ch

Telephone number: +41-21-693 3145

Fax number: +41-21-693 3667

Table of Content

1 Experimental.....	S2
1.1 Chemicals.....	S2
1.2 Two-phase shake flask reactions.....	S2
1.3 Electrospray ionization mass spectrometry (ESI-MS).....	S3
1.4 Water determination by Karl Fischer titration	S4
2 Electrospray ionization mass spectra.....	S5
3 Two-phase shake flask reactions	S7
4 Thermodynamic calculations.....	S8
4.1 Standard redox potentials of oxygen reduction in organic phase	S8
4.2 Two-electron oxygen reduction by DMFc in organic phase.....	S10
5 References.....	S12

1 Experimental

1.1 Chemicals

All chemicals are analytical grade and used as received without further purification. Decamethylferrocene (DMFc, 97%) was purchased from Aldrich. Lithium tetrakis(pentafluorophenyl)borate diethyl etherate (LiTB) was purchased from Boulder Scientific. Sodium iodide (NaI), bis(triphenylphosphoranylidene) ammonium chloride (BACl) and 1,2-dichloroethane (DCE) were obtained from Fluka. 1H-indole was bought from Fluorochem. Bis(triphenylphosphoranylidene) ammonium tetrakis(pentafluorophenyl)borate (BATB) was prepared by metathesis of 1:1 mixtures of BACl and LiTB, in a methanol/water (v/v = 2) mixture, followed by recrystallization in acetone.¹ The aqueous solutions were prepared with ultrapure water (18.2 MΩcm) from a Millipore-Q system.

1.2 Two-phase shake flask reactions

Two-phase shake flask reactions for oxygen reduction were performed in a small flask under stirring. For these experiments, equal volumes (2 mL) of DCE and aqueous solutions containing the reactants were mixed together and stirred vigorously. After reaction, the aqueous and organic phases were separated and the UV/Vis spectrum of the DCE phase was measured directly. The aqueous phase was treated with excess NaI (equivalent to 0.1 M). Hydrogen peroxide reacted with I⁻ to produce I₃⁻, which has an absorbance at 352 nm.² UV/visible (UV/Vis) spectra were obtained with an Ocean Optics CHEM2000 spectrophotometer with a quartz cuvette (path length: 10 mm).

The microelectrode voltammetry measurements were performed with a CHI-900 electrochemical workstation (CH Instruments, Austin, USA) in the traditional three-electrode setup with a commercial glassy carbon microelectrode (13.7 μm diameter, Princeton Applied

Research) working electrode, with a platinum wire and a silver wire as the counter, and quasi-reference electrodes, respectively. The potential scale was referred to the redox couple itself.

The shake-flask experiments for hydrogen evolution were performed in a nitrogen filled glove-box for 16 h. Two-phase reactions were performed in a septum sealed glass vial. The vials with the composition shown in Scheme S1 were prepared in the glove-box. Magnetic stirring (900 rpm) was used to emulsify the two phases for the duration of each experiment. Post-shake flask reaction, 1 mL samples of the headspace gas were obtained using a lock-in syringe with a push-pull valve (SGE Analytical Sciences) in the glovebox and subsequently analyzed by gas chromatography (GC) using a Perkin-Elmer GC (Clarus 400, equipped with 5 Å molecular sieves and an 80/100 mesh) with a thermal conductivity detector (TCD) and argon as a carrier gas.

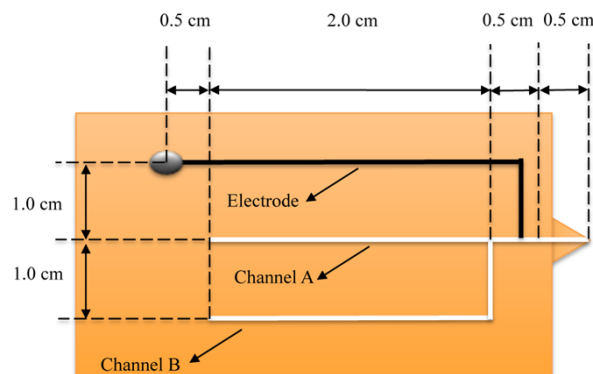
100 μ L H ₂ O 10 mM LiTB 10 mM DMFc 5 mg Mo ₂ C 3 mL DCE a	100 μ L H ₂ O 10 mM DMFc 3 mL DCE b	100 μ L H ₂ O 10 mM DMFc 5 mg Mo ₂ C 3 mL DCE c	100 μ L H ₂ O 10 mM LiTB 5 mg Mo ₂ C 3 mL DCE d
-----------------------------------------------------------------------------------------------------	-------------------------------------------------------------	---------------------------------------------------------------------------------------	---------------------------------------------------------------------------------------

Scheme S1. Schematic representation of the initial compositions for shake-flask experiments under anaerobic conditions. Duration: 16 h.

1.3 Electrospray ionization mass spectrometry (ESI-MS)

A dedicated two-channel microchip was used as an emitter in ESI-MS to analyze the products of the two-phase reactions, shown in scheme S2. Samples taken from the DCE phase were infused via channel A at a flow rate of 60 μ L/h. A sheath flow of ESI buffer (50% water, 49% methanol and 1% acetic acid) was infused via channel B at a flow rate of 60 μ L/h to stabilize ESI performance. High voltage (+3.7 kV) was applied to the electrode to induce ESI. A linear

ion trap mass spectrometer (Thermo LTQ Velos) was used to characterize the emitted ions under positive scanning mode



Scheme S2. Illustration of the two-channel microchip emitter for ESI-MS. The channel A and B each have a cross-section size of $50\ \mu\text{m} \times 100\ \mu\text{m}$. The electrode was made in carbon paste with a cross-section size of $30\ \mu\text{m} \times 100\ \mu\text{m}$.

1.4 Water determination by Karl Fischer titration

The quantity of water in DCE was determined using a Radiometer TitraLab system consisting of a VIT90 Video Titrator, ABU91 Autoburette, and a SAM90 Sample Station. The Karl Fischer solvent was CombiMethanol, and the titrant was CombiTitrant 5, both purchased from Merck. A standard dead-stop end-point titration method was used, where the solvent and its container were titrated dry prior to sample addition to an end-point polarization voltage of a double-platinum electrode to which a constant current was applied. Sample volumes of 1 mL, 2 mL, and 5 mL were titrated, and the determined quantities of water were found to increase in a linear fashion with the sample volume.

2 Electrospray ionization mass spectra

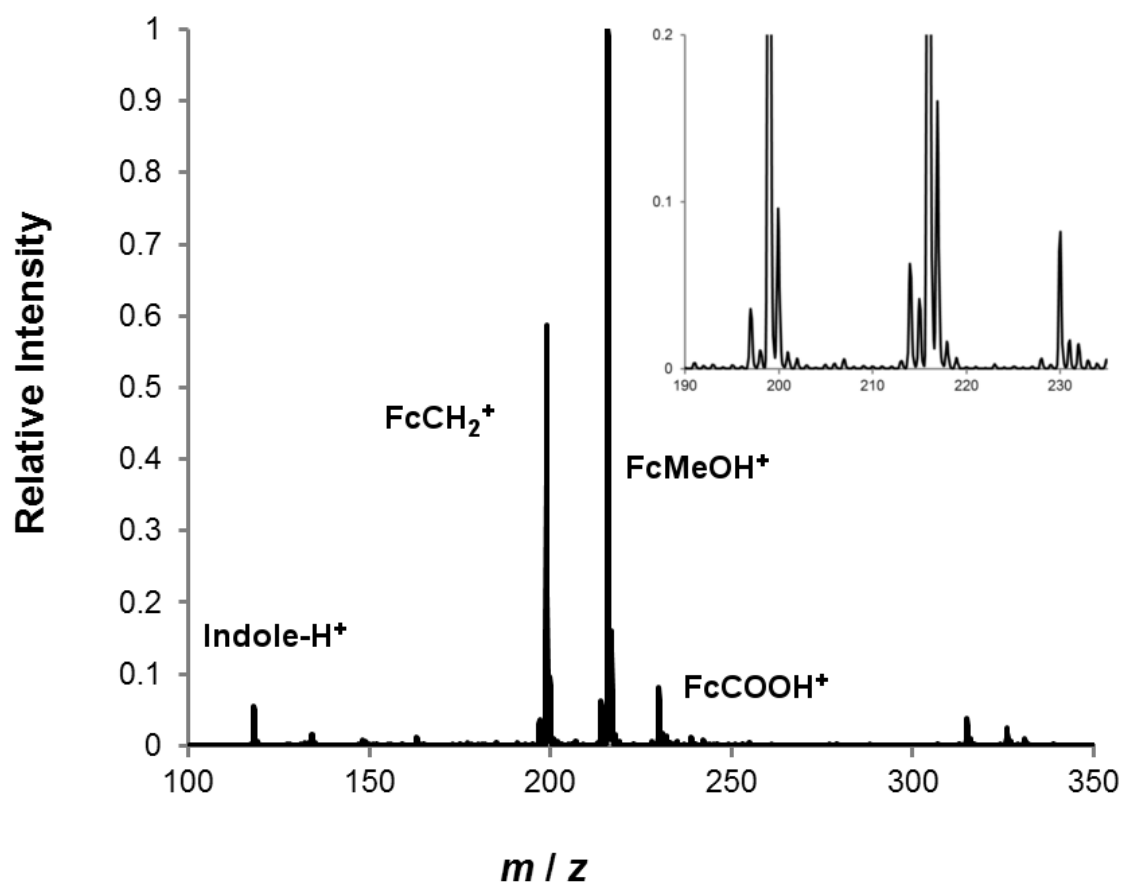


Figure S1. Electrospray ionization mass spectra of 5 mM FcMeOH + 5 mM indole after 30 min at 60°C. The sample was infused via channel A at a flow rate of 60 $\mu\text{L}/\text{h}$. A sheath flow of ESI buffer (50% water, 49% methanol and 1% acetic acid) was infused via channel B at a flow rate of 60 $\mu\text{L}/\text{h}$. Indole- H^+ , protonated indole ion; FcCH₂⁺, α -ferrocenyl carbocation; FcMeOH⁺, oxidized FcMeOH ion with Fe³⁺; FcCOOH⁺, oxidized FcCOOH ion with Fe³⁺.

Figure S1 shows that some FcMeOH ($m / z = 216$) reacted after 30 min to form the corresponding α -ferrocenyl carbocation at $m / z = 199$. Some of the carbocation production may have also been induced by the high voltage of the electrospray. Additionally, small peaks corresponding to protonated indole ($m / z = 118$), FcCOOH ($m / z = 230$) and the reaction product between FcMeOH and indole ($m / z = 315$) are observed. The inset in Figure S1

shows the isotope distribution of the ferrocene species, and the isotope distribution matches the expected distribution for iron containing species.

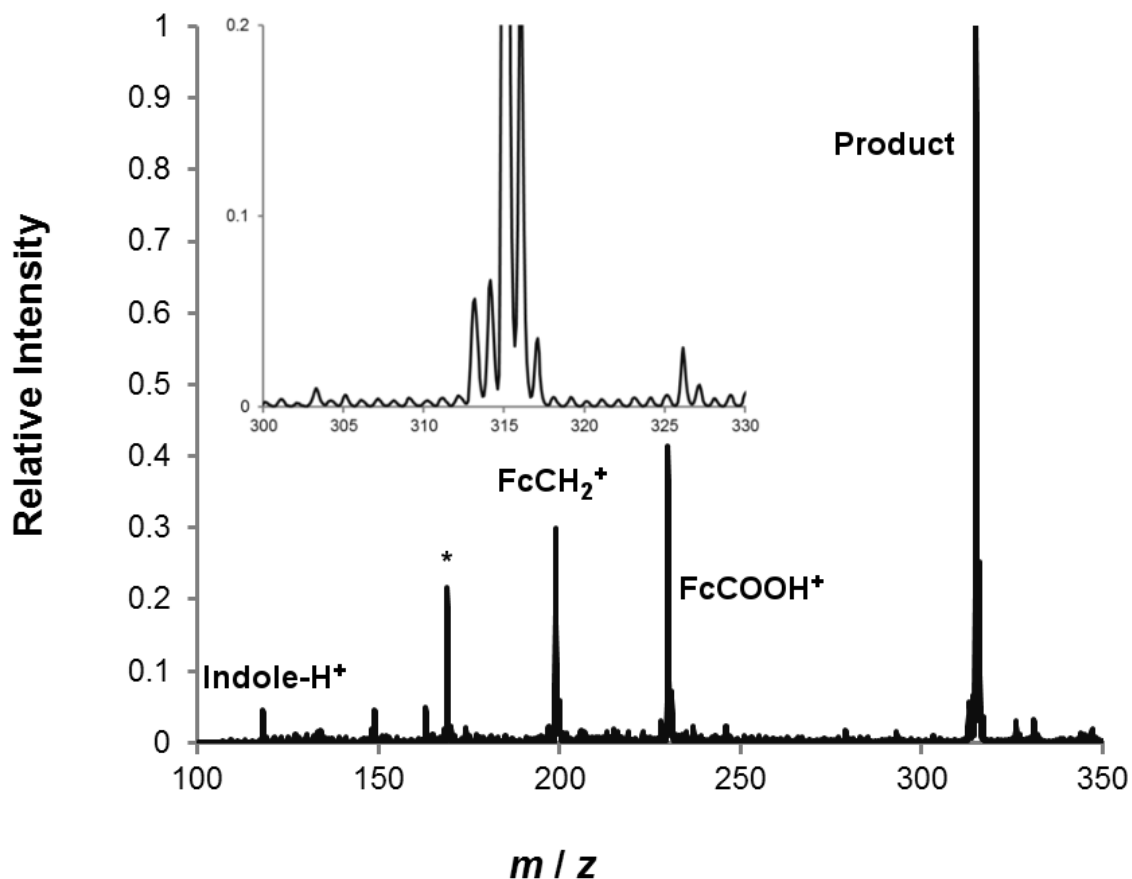


Figure S2. Electrospray ionization mass spectra of 3.33 mM FcMeOH + 3.33 mM indole + 3.33 mM LiTB in DCE after stirring for 30 min at 60°C. The sample was infused via channel A at a flow rate of 60 $\mu\text{L}/\text{h}$. A sheath flow of ESI buffer (50% water, 49% methanol and 1% acetic acid) was infused via channel B at a flow rate of 60 $\mu\text{L}/\text{h}$

Figure S2 shows that after 30 minutes of stirring in the presence of LiTB almost no FcMeOH remains, while the product of the reaction between FcMeOH and indole at ($m/z = 315$) is the most abundant peak; however, some FcCOOH and FcCH₂⁺ are also observed. The peaks around $m/z = 315$ seems to be the mixture of oxidized ions at $m/z = 315$, where the

Fe^{2+} is oxidized to Fe^{3+} under ESI voltage, and protonated ions at $m/z = 316$, where the 3-(ferrocenylmethyl)-1H-indole is protonated at the nitrogen. The unidentified peak at 169 Th does not have the isotope distribution of iron, and it is assumed to be a decomposition product from carbon paste used for the ESI microchip. After the experiments with additional samples in DCE, the microchip showed signs of delamination, and some of the carbon paste electrode had dissolved in DCE influencing the ESI-MS analyses.

3 Two-phase shake flask reactions

The UV/Vis spectra and microelectrode voltammograms of the vials in Figure 1 of the main text after 140 min reaction.

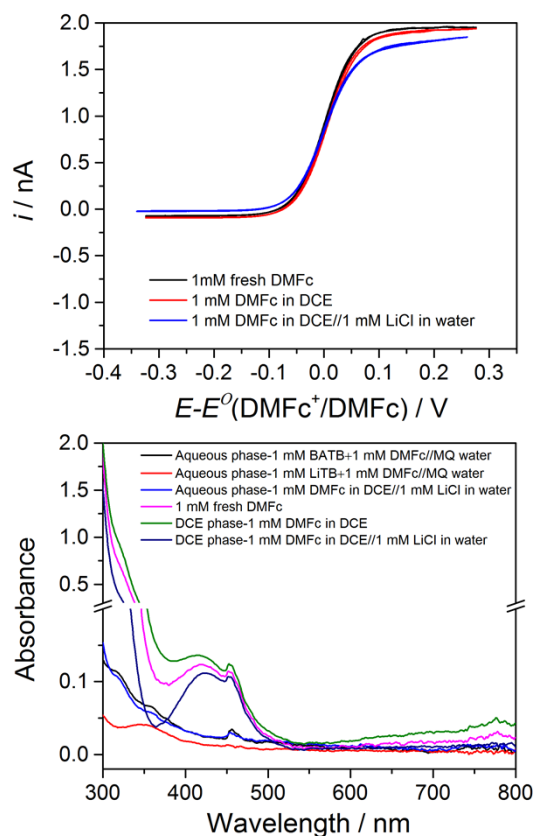


Figure S3. The glassy carbon UME (13.7 μm diameter) CVs (10 mV s^{-1}) for the DCE phases and the UV/Vis spectra for aqueous (treated by 0.1 M NaI beforehand) and DCE phases specified in the Figure 1 of the main text after shake-flask reactions.

4 Thermodynamic calculations

4.1 Standard redox potentials of oxygen reduction in organic phase

The standard redox potentials of the reactions in DCE can be estimated by the thermodynamic cycle.³ Generally, a half reaction for the reduction of O to R in phase α can be expressed as:



With the standard redox potential in the Standard Hydrogen Electrode scale expressed as:

$$[E_{\text{O/R}}^0]_{\text{SHE}}^\alpha = \frac{\Delta G^0}{-nF} = \frac{1}{nF} \left[\mu_{\text{O}}^{0,\alpha} - \mu_{\text{R}}^{0,\alpha} - n \left(\mu_{\text{H}^+}^{0,\text{w}} - \frac{1}{2} \mu_{\text{H}_2}^{0,\text{w}} \right) \right] \quad (\text{SI } 2)$$

Where F is the Faraday constant. The standard redox potentials of the reaction in DCE and aqueous are:

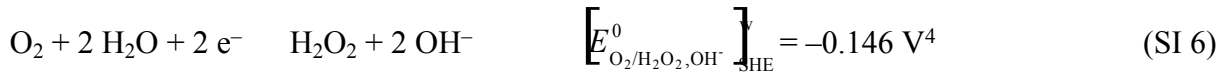
$$[E_{\text{O/R}}^0]_{\text{SHE}}^{\text{DCE}} = \frac{1}{nF} \left[\mu_{\text{O}}^{0,\text{DCE}} - \mu_{\text{R}}^{0,\text{DCE}} - n \left(\mu_{\text{H}^+}^{0,\text{w}} - \frac{1}{2} \mu_{\text{H}_2}^{0,\text{w}} \right) \right] \quad (\text{SI } 3)$$

$$[E_{\text{O/R}}^0]_{\text{SHE}}^{\text{w}} = \frac{1}{nF} \left[\mu_{\text{O}}^{0,\text{w}} - \mu_{\text{R}}^{0,\text{w}} - n \left(\mu_{\text{H}^+}^{0,\text{w}} - \frac{1}{2} \mu_{\text{H}_2}^{0,\text{w}} \right) \right] \quad (\text{SI } 4)$$

If equation SI 3 is subtracted from equation SI 4, then we can obtain equation SI 5 shown below:

$$\begin{aligned} [E_{O/R}^0]_{SHE}^{DCE} &= [E_{O/R}^0]_{SHE}^W + \frac{1}{nF} [\mu_O^{0,DCE} - \mu_O^{0,W} + \mu_R^{0,W} - \mu_R^{0,DCE}] \\ &= [E_{O/R}^0]_{SHE}^W + \frac{1}{nF} (\Delta_O^W G_O^{0,W \rightarrow DCE} - \Delta_O^W G_R^{0,W \rightarrow DCE}) \end{aligned} \quad (SI 5)$$

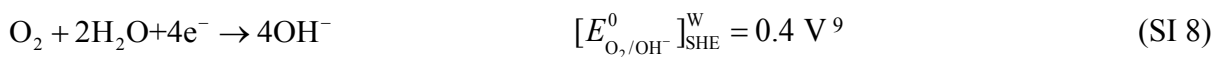
Where $\Delta_{DCE}^W G_i^{0,W \rightarrow DCE}$ is the standard Gibbs transfer energy of species i from the aqueous to DCE phase. For the case of the two-electron reduction:



$$\begin{aligned} \left[E_{O_2/H_2O_2, OH^-}^0 \right]_{SHE}^{DCE} &= \left[E_{O_2/H_2O_2, OH^-}^0 \right]_{SHE}^W + \\ &\frac{1}{2F} (\Delta_{DCE}^W G_{O_2}^{0,W \rightarrow DCE} + 2\Delta_{DCE}^W G_{H_2O}^{0,W \rightarrow DCE} - \Delta_O^W G_{H_2O_2}^{0,W \rightarrow DCE} - 2\Delta_{DCE}^W G_{OH^-}^{0,W \rightarrow DCE}) \end{aligned} \quad (SI 7)$$

$\Delta_{DCE}^W G_{O_2}^{0,W \rightarrow DCE}$ was calculated as $-3.99 \text{ kJ mol}^{-1}$ based on solubility of oxygen in water (0.27 mM)⁵ and DCE (1.4 mM)⁶, $\Delta_{DCE}^W G_{H_2O}^{0,W \rightarrow DCE}$ was calculated as $15.42 \text{ kJ mol}^{-1}$ based on solubility of water in DCE (1846 ppm)⁷ and the same value was used for $\Delta_{DCE}^W G_{H_2O_2}^{0,W \rightarrow DCE}$ as an approximation, as described previously.³ The standard Gibbs transfer energy of OH^- from water to DCE ($G_{OH^-}^{0,W \rightarrow DCE}$) is 63.3 kJ mol^{-1} .⁸ Finally, this calculations gives a standard redox potential of $\left[E_{O_2/H_2O_2, OH^-}^0 \right]_{SHE}^{DCE} = -0.74 V$.

For the four-electron oxygen reduction, we have:



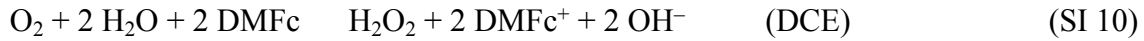
$$\left[E_{\text{O}_2/\text{OH}^-}^0 \right]_{\text{SHE}}^{\text{DCE}} = \left[E_{\text{O}_2/\text{OH}^-}^0 \right]_{\text{SHE}} + \frac{1}{4F} (\Delta_{\text{DCE}}^{\text{W}} G_{\text{O}_2}^{0, \text{W} \rightarrow \text{DCE}} + 2\Delta_{\text{DCE}}^{\text{W}} G_{\text{H}_2\text{O}}^{0, \text{W} \rightarrow \text{DCE}} - 4\Delta_{\text{DCE}}^{\text{W}} G_{\text{OH}^-}^{0, \text{W} \rightarrow \text{DCE}}) \quad (\text{SI } 9)$$

Using the same values as previously the result is $\left[E_{\text{O}_2/\text{OH}^-}^0 \right]_{\text{SHE}}^{\text{DCE}} = -0.185 \text{ V}$.

4.2 Two-electron oxygen reduction by DMFc in organic phase

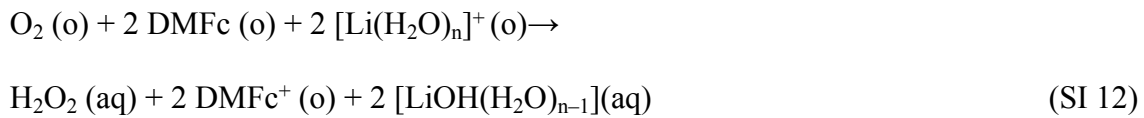
If DMFc was used as the reducing agent, the standard Gibbs energy change of electron transfer ΔG_{et}^0 of the chemical reaction SI 10 is given by equation SI 11, where

$\left[E_{\text{DMFc}^+/\text{DMFc}}^0 \right]_{\text{SHE}}^{\text{DCE}}$ is 0.04 V ,¹⁰



$$\Delta G_{\text{et}}^0 = -2F \left(\left[E_{\text{O}_2/\text{H}_2\text{O}_2, \text{OH}^-}^0 \right]_{\text{SHE}}^{\text{DCE}} - \left[E_{\text{DMFc}^+/\text{DMFc}}^0 \right]_{\text{SHE}}^{\text{DCE}} \right) = 151 \text{ kJ mol}^{-1}. \quad (\text{SI } 11)$$

In the case of the two-electron reduction, the overall reaction described by Eq. 4-6 in the main text is:

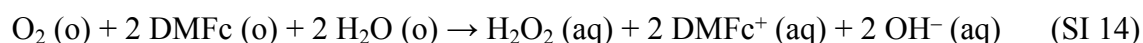


The total Gibbs free energy change for oxygen reduction by DMFc (equation SI 12) is then (the transfer energies of Li^+ and OH^- were taken as 59.8 kJ mol^{-1} and 63.3 kJ mol^{-1} , and these experimental values include the transfer of the n water molecules on the hydration shell of the ion)⁸

$$\Delta G_{\text{tot}}^0 = \Delta G_{\text{et}}^0 - \Delta_{\text{DCE}}^{\text{W}} G_{\text{H}_2\text{O}_2}^{0, \text{W} \rightarrow \text{DCE}} - 2\Delta_{\text{DCE}}^{\text{W}} G_{\text{Li}^+}^{0, \text{W} \rightarrow \text{DCE}} - 2\Delta_{\text{DCE}}^{\text{W}} G_{\text{OH}^-}^{0 \text{W} \rightarrow \text{DCE}} = -110.6 \text{ kJ mol}^{-1}$$

(SI 13)

If no lithium is present in the oil phase, the produced DMFcOH will transfer into the aqueous phase ($\Delta_{\text{DCE}}^{\text{W}} G_{\text{DMFc}^+}^{0, \text{W} \rightarrow \text{DCE}} = 24.1 \text{ kJ mol}^{-1}$):



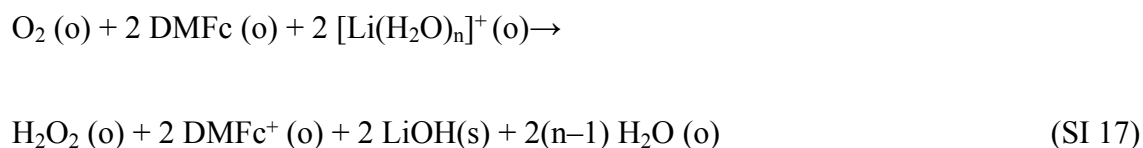
$$\Delta G_{\text{tot}}^0 = \Delta G_{\text{et}}^0 - \Delta_{\text{DCE}}^{\text{W}} G_{\text{H}_2\text{O}_2}^{0, \text{W} \rightarrow \text{DCE}} - 2\Delta_{\text{DCE}}^{\text{W}} G_{\text{DMFc}^+}^{0, \text{W} \rightarrow \text{DCE}} - 2\Delta_{\text{DCE}}^{\text{W}} G_{\text{OH}^-}^{0 \text{W} \rightarrow \text{DCE}} = +57.3 \text{ kJ mol}^{-1}$$

(SI 15)

In the case where there is no separate aqueous phase LiOH formed in the reaction will precipitate. The Gibbs free energy of solvation of LiOH in DCE was calculated from a thermodynamic cycle by the following procedure:

$$\Delta G_{\text{sol, LiOH}}^{\text{DCE}} = \Delta G_{\text{sol, LiOH}}^{\text{W}} + \Delta_{\text{DCE}}^{\text{W}} G_{\text{Li}^+}^{0, \text{W} \rightarrow \text{DCE}} + \Delta_{\text{DCE}}^{\text{W}} G_{\text{OH}^-}^{0 \text{W} \rightarrow \text{DCE}} \quad (\text{SI 16})$$

$\Delta G_{\text{sol, LiOH}}^{\text{W}}$ was calculated from the solubility product ($\ln K_{\text{sp}}$ at 293.15 K = 3.312)¹¹ as $-8.07 \text{ kJ mol}^{-1}$, and hence $\Delta G_{\text{sol, LiOH}}^{\text{DCE}} = 115 \text{ kJ mol}^{-1}$. The total Gibbs free energy for the reaction (SI 17) is then



$$\Delta G_{\text{tot}}^0 = \Delta G_{\text{et}}^0 - 2\Delta G_{\text{sol, LiOH}}^{\text{DCE}} = -78.9 \text{ kJ mol}^{-1} \quad (\text{SI 18})$$

The results summarized in Table S1 indicate that oxygen reduction to hydrogen peroxide in the DCE phase followed by transfer of DMFcOH into the aqueous phase is not thermodynamically favorable, but all the other reactions are significantly exergonic.

Table S1. Summary of the thermodynamic calculations of the oxygen reduction by DMFc in the DCE phase in different conditions.

Conditions	ΔG_{tot}^0 , kJ mol ⁻¹
Li ⁺ in oil phase, LiOH transfers	-111
Li ⁺ in oil phase, LiOH precipitates	-78.9
No Li ⁺ in oil phase, DMFcOH transfers	57.3

5 References

1. D. J. Fermín, H. D. Duong, Z. Ding, P. F. Brevet and H. H. Girault, *Phys. Chem. Chem. Phys.*, 1999, **1**, 1461-1467.
2. B. Su, R. Partovi-Nia, F. Li, M. Hojeij, M. Prudent, C. Corminboeuf, Z. Samec and H. H. Girault, *Angew. Chem., Int. Ed.*, 2008, **47**, 4675-4678.
3. I. Hatay, B. Su, F. Li, M. A. Méndez, T. Khoury, C. P. Gros, J. M. Barbe, M. Ersoz, Z. Samec and H. H. Girault, *J. Am. Chem. Soc.*, 2009, **131**, 13453-13459.
4. P. Vanýsek, in *CRC Handbook of Chemistry and Physics, 94th Ed., Internet Version*, ed. W. M. Haynes, CRC Press, Boca Raton, 2014.
5. R. Battino, T. R. Rettich and T. Tominaga, *J. Phys. Chem. Ref. Data*, 1983, **12**, 163-178.
6. P. Luehring and A. Schumpe, *J. Chem. Eng. Data*, 1989, **34**, 250-252.
7. A. Trojánek, J. Langmaier and Z. Samec, *Electrochim. Acta*, 2012, **82**, 457-462.
8. M. Zhou, S. Gan, L. Zhong, X. Dong, J. Ulstrup, D. Han and L. Niu, *Phys. Chem. Chem. Phys.*, 2012, **14**, 3659-3668.

9. A. J. Bard and L. R. Faulkner, *Electrochemical Methods*, 2nd edn., John Wiley & Sons, New York, 2001.
10. I. Hatay, B. Su, F. Li, R. Partovi-Nia, H. Vrubel, X. Hu, M. Ersoz and H. H. Girault, *Angew. Chem., Int. Ed.*, 2009, **48**, 5139-5142.
11. C. Monnin and M. Dubois, *J. Chem. Eng. Data*, 2005, **50**, 1109-1113.